Journal of
Iberian Geology
AN INTERNATIONAL PUBLICATION OF EARTH SCIENCES

Anthropogenic influence in the Sado estuary (Portugal): a geochemical approach

Influencia antrópica en el estuario de Sado (Portugal): una aproximación geoquímica

M.C. Freitas[1], C. Andrade[1], A. Cruces[1], J. Munhá[1], M. J. Sousa[2], S. Moreira[1],
J. M. Jouanneau[3], L. Martins[1]

[1]*Centro e Departamento de Geologia, Faculdade de Ciências, Universidade de Lisboa, Bloco C6, 3° piso, Campo Grande, 1749-016 Lisboa, Portugal; Fax: +351 217500119; cfreitas@fc.ul.pt; candrade@fc.ul.pt; a.cruces@fc.ul.pt; jmunha@fc.ul.pt; sccm@netvisao.pt; lmartins@fc.ul.pt*
[2]*Departamento de Ciências da Terra e Centro de Investigação em Geociências Aplicadas, FCT/UNL, Campus de Caparica, 2829-516 Caparica, Portugal; geojotas@ciga.fct.unl.pt*
[3]*Département Géologie et Océanographie, UMR 5805, CNRS, Univ. Bordeaux I, Avenue des Facultés, 33405 Talence Cedex, France; jm.jouanneau@epoc.u-bordeaux1.fr*

Abstract

Two areas of salt marsh in the Sado estuary – Faralhão, on the industrialized north margin and Malha da Costa, on the south bank, sheltered by a uninhabited sand spit – have been cored to study the geochemical signature of anthropogenic activity in recent (19th century onwards) intertidal sediments. Short cores were taken from each site from both the high and low marsh and were studied for texture, organic matter, pH, carbonates and geochemistry, including the heavy metals Cu, Pb and Zn. The marsh sediments are free of carbonate bioclasts and quite uniform in texture, consisting of acid to neutral clayey silt in addition to organic matter, which is higher in the top 20 cm.

The vertical concentration profiles of heavy metals indicates enrichment in the top 30 cm of the sediment of the high marsh, in contrast with underlying high and low marsh sediment that has concentrations of metals at both studied sites similar to the Average Shale international reference/ continental crust sediments. The geochemical signal of anthropogenic influence in the marsh sediment was determined to have commenced from 1900-1920 using the sedimentation rates derived from ^{210}Pb and ^{137}Cs analyses. Spatial contrast in contamination levels was found within the estuary, with sediments of the Faralhão marsh showing higher enrichment factors of all metals. The anthropogenic increase of the supply of metal to the Sado estuary resulted from extensive exploitation of pyrite ore in the drainage basin until the1960's; since that time, the sediments record a break in metal input, which resulted from a decline of the mining industry. However, in the marsh located closer to the industrial area (Faralhão) this break is followed by a local increase of heavy metal fluxes, which is interpreted as the result of intensification of anthropogenic influence. The comparison of metal concentrations in marsh sediments with target values established in quality guidelines indicates the studied area to be of environmental concern.

Keywords: salt-marsh, heavy metals, sedimentation rates, pollution.

Resumen

Con el fin de estudiar el registro geoquímico de la actividad antrópica en sedimentos recientes (a partir del siglo XIX) e intermareales, han sido perforadas dos zonas de marisma en el Estuario del Sado- Faralhão, en el industrializado margen norte, y Malha da Costa, en la orilla sur, resguardada por una flecha litoral de arena no ocupada antrópicamente. Los pequeños sondeos realizados en cada punto de muestreo englobaron la marisma alta y baja. Fueron realizados análisis texturales, de contenido en materia orgánica, de pH, carbonatos y geoquímica, incluyendo los metales pesados Cu, Pb y Zn. Los sedimentos de marisma no muestran carbonato bioclástico y son bastante uniformes en la textura, consistiendo en limo arcilloso ácido a neutro junto con materia orgánica cuyo contenido es mayor en los 20 cm más superficiales.

La concentración vertical de los perfiles de metales pesados indica un enriquecimiento en los 30 cm superficiales de la marisma alta, en contraste con los sedimentos subyacentes de marisma alta y baja que poseen concentraciones de metales similares a los referenciados internacionalmente para Average Shale / sedimentos de corteza continental. La señal geoquímica de la influencia antrópica en los sedimentos de marisma fue datada de 1900 a 1920 usando las tasas de sedimentación deducidas mediante ^{210}Pb y ^{137}Cs. Un contraste espacial en los niveles de contaminación fue encontrado en el interior del estuario: la marisma de Faralhão muestra valores con mayor enriquecimiento para todos los metales. El aporte antrópico de metales en el estuario de Sado resulta de la extensa explotación de pirita en la cuenca hasta 1960; a partir de ese momento los sedimentos registran una disminución en el aporte antropogénico de metales, consecuencia de la disminución del trabajo minero. Sin embargo, en la marisma cercana a la zona industrial (Faralhão) a esta interrupción le sigue un restablecimiento del flujo de metales pesados, interpretado como resultado del aumento de la influencia antrópica. La comparación de las concentraciones de metales en sedimentos de marisma con valores fijados establecidos en directrices de calidad sugiere una inquietud ambiental para el área de estudio.

Palabras clave: marisma, metales pesados, tasas de sedimentación, polución.

1. Introduction

Estuaries are complex transitional environments supporting valuable and specific biota and are a focal point of a varied suite of human activities and demands – commerce, manufacturing industry, fisheries, leisure pursuits and conservation of landscape or wildlife – that are often in conflict and may produce environmental degradation. The increase of environmental awareness and the need to assess and improve environmental quality has led societies to encourage research and produce legislation to promote the sustainability of these environments; in this respect Portugal should be no exception.

One of the main environmental problems of estuaries is enrichment in heavy metals that accumulate preferably in fine grained and, especially organic, sediments which constitute an excellent archive for the reconstruction of the pattern of metal concentrations with time. Heavy metals may have both natural (continental or marine) and anthropogenic origins, the latter modifying the natural fluxes. The assessment of human influence requires the knowledge of natural concentrations (background levels used as reference values), which have preferably been obtained locally or regionally. In addition, the changes in metal concentration related to sediment compositional and textural variability must be considered in order to normalize criteria for evaluation of sediment quality in terms of contamination.

Despite the large amount of published work on heavy metal concentration and distribution in recent Portuguese estuarine sediments, including the Sado estuary (Pêra *et al.*, 1977; Vale and Sundby, 1980; Quevauviller *et al.*, 1989; Cortesão and Vale, 1995; IH, 1999, 2000; Belchior *et al.*, 2000), few characterized the natural inputs to the system. This paper decribes the character of the sediment deposited in the salt marshes of the Sado estuary since the middle 19th century, as well as their pre- and post-industrial geochemical signatures.

2. The study area

The Sado estuary is a barred estuary on the western Portuguese coast, circa 40 km south of Lisbon (Fig. 1). It is the second largest estuary in Portugal and one of the most important estuaries in Europe. The Sado estuary constitutes a shallow basin, with an average depth of 8 m with a maximum depth of 50 m in the inlet channel. The area flooded at high water is of about 150 km^2 and extends NW-SE upstream for 37.5 km to Alcácer do Sal and in a NNE-SSW direction for 25 km to between Águas de Moura and Comporta (Fig. 1). The tidal inlet, circa 2 km wide, is constrained by the northern extreme of the Tróia sand spit and the Arrábida mountain and its narrow entrance prevents the propagation of oceanic waves into the inner estuary. The inlet channel bifurcates upstream into the Canal Norte (flood-dominated) and Canal Sul (ebb-dominated), which are separated by several aligned sand shoals.

The Sado estuary is high-mesotidal, the tidal amplitude varying between 1.3 m during neap tides and 3.5 m at
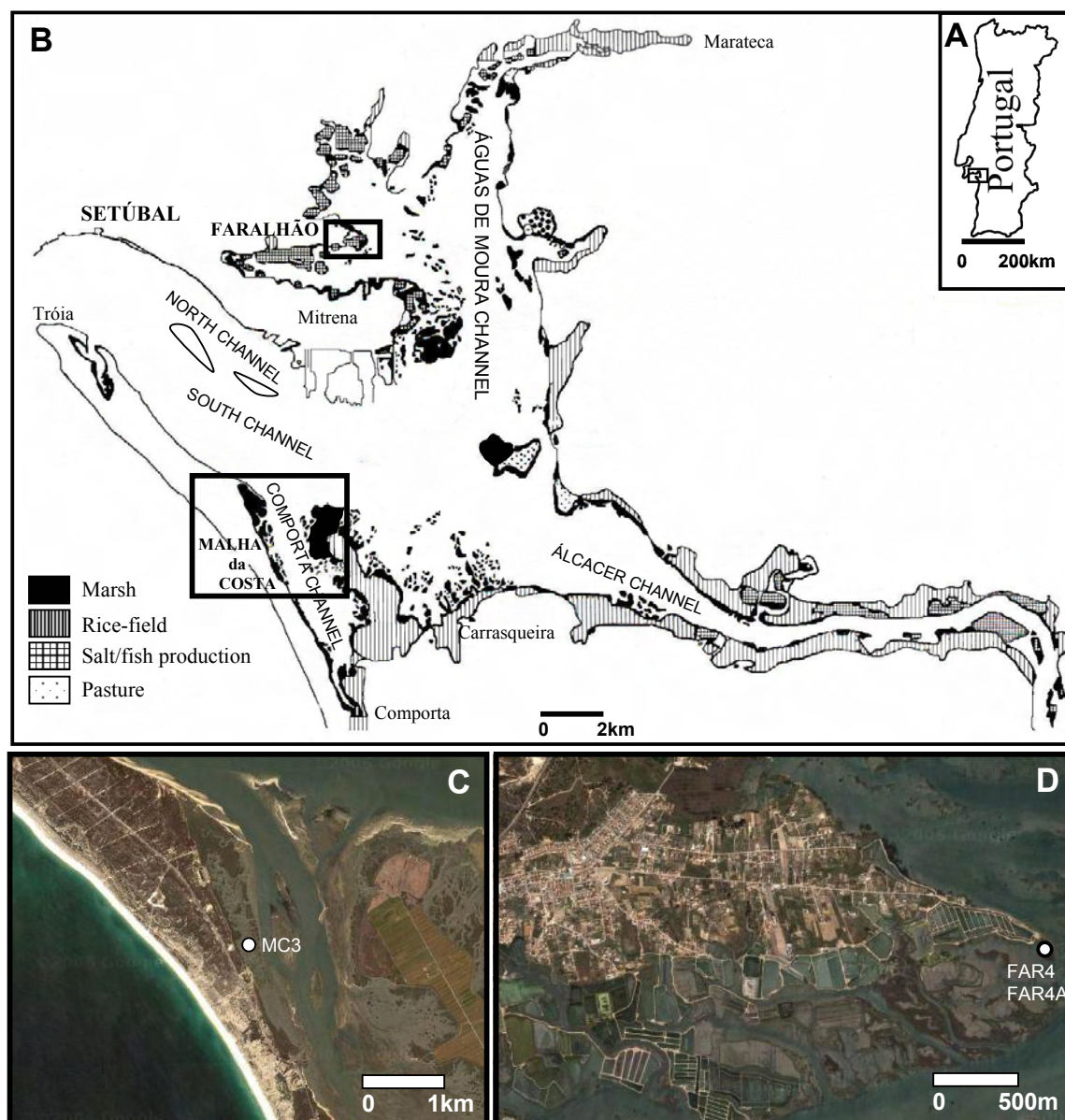
Fig. 1.– The Sado estuary. A- Location. B – Distribution of marsh and anthropogenic occupation of estuarine margins. C and D – Location of coring sites Faralhão and Malha da Costa (satellite image from Google maps, 2007).

Fig. 1.– Estuario de Sado. A. Localización en Portugal. B. Distribución de marismas y ocupación antrópica de los margenes del estuario. C. y D. Situación de los sondeos localizados en Faralhão y Malha da Costa (imagen de satélite de Google-mapas, 2007).

spring water, near the mouth; the tidal range increases upstream, to reach a maximum of 4.14 m at mean high water spring tide (MHWS) at Montalvo, 26 km inland. The spring tidal prism is 3.8×10^6 m³ and tidal currents dominate the estuarine dynamics, given the limited fresh-water discharge of the Sado River and the negligible streamflow of the small Marateca and Comporta rivers. Consequently, the salinity remains close to normal marine water (slightly above 30‰) and a significant part of the estuarine floor is covered by sandy sediments of marine origin. Suspended material within the interior drainage basin settles preferably in sheltered, low energy regions,

along the estuarine margins, where mud flats and salt marshes have accumulated. The inner estuarine intertidal flats accrete at about 10 mm/year (Andrade *et al.*, 2006), exceeding the 1-2 mm/year rate of rise of mean sea level (MSL) (Dias and Taborda, 1992); in contrast, the width of the marginal salt marshes decreased circa 17 cm/year in the late 20th century (Moreira, 1992).

Human occupation of the estuarine margins is intense, diverse and highly asymmetric. The north margin of the lower estuary is under intense anthropic stress associated with the city of Setúbal (one of the main Portuguese commercial and fishing ports) and nearby extensive in-

dustrial facilities (paper mills, chemical fertilizers, pesticides, herbicides, fungicides, other biochemical products, metal processing, shipyards, thermo-electrical production, plastic components and packing, car repair works) that are mainly concentrated in the Mitrena peninsula; the remainder of the north and the south margin are areas of both agricultural activities (with relevance to rice production) and fish farming (both have been developed on former salt marshes), as well as a few leisure resorts (located on the Tróia spit).

The Sado River has a 7692 km² drainage basin, with outlets in the SE segment of the estuary. Contrasting with the estuarine margins, most of the drainage basin is largely uninhabited and is an area of agricultural and forest activities. Industry occupies less than 1% of the surface area and consists of cattle raising and food production. Pig farms, olive oil facilities and fish processing units are important for the local economy and may constitute point-sources of pollution. In addition, a large number of sites of mineral exploitation are scattered throughout the drainage basin. These have been extracting and processing massive sulphide poly-metallic ore since the late 19th - mid 20th century for sulfur, zinc, lead, copper, iron and manganese. There was an earlier pulse in mining activity which dates from the Roman times, when the residual/supergenic enrichment zone of ore accumulations were exploited for gold, silver and copper. These mines have experienced prolonged periods of abandonment/non-activity and their tailings constitute local sources of heavy metals for surface and ground water, which are eventually flushed out into the Sado estuary. The assessment and control of the contamination potential and the yields of industry has been growing recently, not only due to legal impositions, but also as a consequence of the necessity of the maintenance of environmental quality standards required by certification agencies and European funding programmes.

In the Sado estuary, two of the most important salt marsh areas, located on the northern (Faralhão – FAR) and southern (Malha da Costa – MC) margins, have been chosen for this study.

The present-day FAR marsh represents the remains of a much larger area that has been drained and filled to accommodate the growth of Faralhão village and reclaimed for salt production and fish farming (Fig. 1). The marsh environment consists essentially of high marsh colonized by *Halimione portucaloides*, *Arthrocnemum fruticosum*, *Suaeda vera*, *Limonium vulgare*, *Inula crithmoides* and *Puccinelia maritima* (Sousa, 2006) and by a fringing and patchy low marsh with *Spartina maritima*. The horizontal junction between both marsh types or between the high marsh and the adjacent intertidal flat is often formed by a scarp (Fig. 2). The surface of the high marsh is fairly hori-
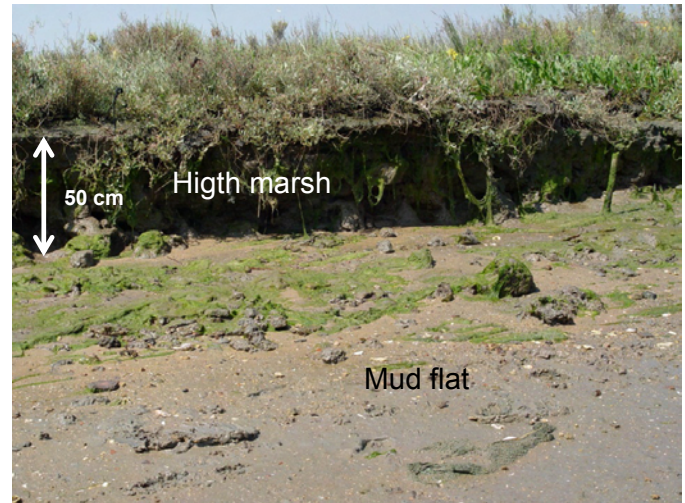

Fig. 2.– The scarped junction between high marsh and mudflat at Faralhão saltmarsh.
Fig. 2.– Transición abrupta entre la marisma alta y la llanura de inundación mareal en las marisma de Faralhão
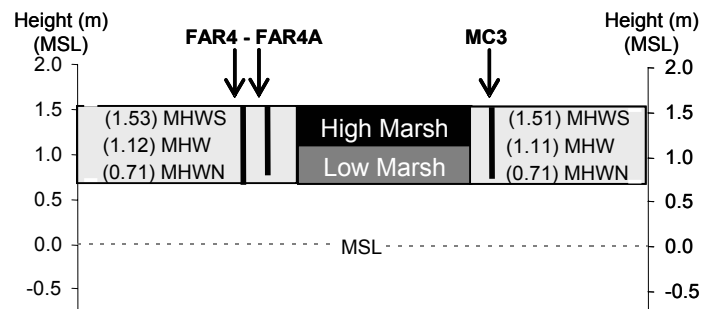

Fig. 3.– The vertical range of sedimentary cores in relation to tidal elevations at both sites.
Fig. 3.– Rango vertical de los sondeos sedimentarios enmarcado dentro de las elevaciones mareales en ambos márgenes

zontal and reaches up to 4 cm below MHWS (1.53 m MSL); the surface of the low marsh is more irregular and roughly extends from local Mean High Water (1.12 m MSL) to local Mean High Water Neap (0.71 m MSL) – Fig. 3; these limits are similar to marsh elevation ranges referred in the literature (e.g. Davis and FitzGerald, 2004).

The MC marsh is an elongated area fringing the estuarine margin of the Tróia sand spit, confined by the toe of the barrier dune complex and protected by the sandy linear bars of the Canal Sul. The MC marsh represents a dissected, mature high marsh that contains frequent salt pans, separated from the intertidal mudflat by a retreating scarp. The low marsh is reduced to scattered and discontinuous patches, which are concentrated close to the main channel. The dominant vegetation is similar to that of FAR. Again, the surface of the high marsh is fairly horizontal though more irregular than that of FAR and the mean elevation (1.55 m MSL) reaches to 4 cm above local Mean High Water Spring (1.51 m MSL) – Fig. 3.

3. Methods

A 84 cm-long core (FAR4) and another 76 cm-long replica (FAR4A) were collected from the high marsh in 2003 and in 2005, respectively, from the north bank of Águas de Moura channel, at Faralhão (Fig. 1) using a van der Horst sampler. Core FAR4A was sub-sampled at each cm interval; 75 samples were analyzed for water content and pH and 39 samples were studied for other sedimentological parameters. Core FAR4 was used for geochemical analysis; 13 samples of the bulk sediment have been chosen in the upper part of the core (0-34 cm) for ^{210}Pb and ^{137}Cs determination; these and up to ten additional samples, taken from the lower part, were processed for elemental analysis.

A 78 cm-long core (MC3) was also taken from the high marsh in 2003 on the south margin of Comporta channel, at Malha da Costa, (Fig. 1) using the same sampler. This core has been sub-sampled irregularly at 1 to 2 cm interval. A total of 52 samples were analysed for pH and 21 for other sedimentological parameters. Twelve samples have been chosen in the upper part of the MC3 core (0-41 cm) for ^{210}Pb and ^{137}Cs determination; these and four additional samples, taken from the lower part, were processed for elemental analysis.

Water content was measured by weight difference (after 48 hours of oven-drying at 60ºC) in relation to weight of dry sediment. Sediment pH was determined using the electrometric method (Head, 1980) and classified following Pratolongo (in Costa, 1999). Organic matter (OM) content of the sediment was determined for the total sample using about 1g of dry sediment by oxidation with K-dichromate followed by titration using Fe-sulphate (Standard E-201 - LNEC, 1967). The calcium carbonate content was evaluated approximately by inspection of the reaction of the sediment with diluted HCl (all sediments were found carbonate free). Wet sieving was used to separate and determine the ratio of coarse (>63μm): fine (<63μm) particles and the silt and clay fractions were determined using a Malvern laser particle analyzer. The textural classification of the sediments follows Flemming (2000). The natural excess of ^{210}Pb and radionuclide ^{137}Cs concentrations was determined by γ spectrometry. Major (Al, Ca, Fe, K, Mg, Mn, Na, Ti) and minor (Cu, Pb and Zn) elemental contents were determined using flame atomic absorption spectrometry; in addition, Si was analyzed by the classic gravimetric method. Volatile contents of samples processed for geochemistry were measured by loss on ignition (700-800ºC, 30 min) – LOI. The heavy metal contents were normalized in relation to Al and LOI to minimize textural and compositional effects. The enrichment factor (EF) of metals in the upper section (us) of the cores was calculated in relation to the average concentrations found in the lower section (ls), which were taken as the local pre-industrial background reference using FE= ([Metal]$_{us}$ / [LOI or Al]$_{us}$)/ ([Metal]$_{ls}$ / [LOI or Al]$_{ls}$) (Loring and Rantala, 1992).

Heavy metal (M_i: i = Cu, Pb, Zn) contents ($\mu gM_i.g_{sediment}^{-1}$) in excess of those of their respective average background values (discussed below) are defined as "excess c(M_i)" = $\Delta c(M_i)_z$ = c(M)$_z$ – c$_{average\ background}$ (M_i)$_{z \leq us/ls\ boundary\ depth}$, for each sample at z = - *cm* depth within the upper section of the cores. $\Delta c(M_i)_z$ values were fitted to appropriate polynomial functions $F(z) = \Delta c(M_i)_z$ (describing down core variations in excess M_i contents) and coupled with calculated sedimentation rates ($SR(z)$ = -dz/dt: cm.year^{-1}; detailed below) in order to estimate anthropogenic contributions to metal fluxes into the sedimentary budget. Thus, at each time t (= t_0 - $\Delta z/SR(z)$; t_0 = 1900-1920, $z_0 \approx$ - 30 cm, at the lower boundary of the upper section of the studied cores), (dG/dz)$_t$ ($G = F(z)/\rho_{sediment}$; $\rho_{sediment}$ = average sediment density ≈ 1 g.cm^{-3}) describes the rate of variation of excess heavy metal input, per cm sediment deposited, over an area of 1 cm². As a first approximation, it is assumed that geochemical features of core samples are representative of sediments within each of the studied areas, ~ 1 km², and (dG/dz)$_t$ values were multiplied by 10^4 (μg = 10^{-6} g; km² = 10^{10} cm²) to obtain excess heavy metal flux units of gM$_i$.cm$_{sediment\ deposited}^{-1}$.km², as shown in figure 14.

Factor analysis (R mode) was applied to a series of 13 geochemical variables in order to extract the main factors that influence the distribution of Al, Si, Ca, Fe, K, Mg, Mn, Na, Ti,Cu, Pb and Zn, along 17 and 15 samples in cores FAR4 and MC3, respectively. Factor loadings and subsequent Varimax raw rotation were extracted through a STATISTICA 7 software package. Factor 1 and 2 were considered significant, with relative importance of 40 and 12% (52% total variance explained), respectively for FAR4 and 49 and 12% (61% total variance explained) for MC3.

4. Results and Discussion

Cores taken from both sample sites extend almost entirely throughout the elevation range of the high and the low marsh depositional environments; the former corresponds approximately to the upper 40 cm of sediment (Fig. 3).

4.1. Sedimentology

The low marsh (76 – 40 cm at FAR4A and 78 - 44 cm at MC3) consists essentially of slightly clayey silt (<63μm fraction exceeding 99%), with the silt fraction representing 75-80% of the total sediment (Fig. 4A, B). The mean
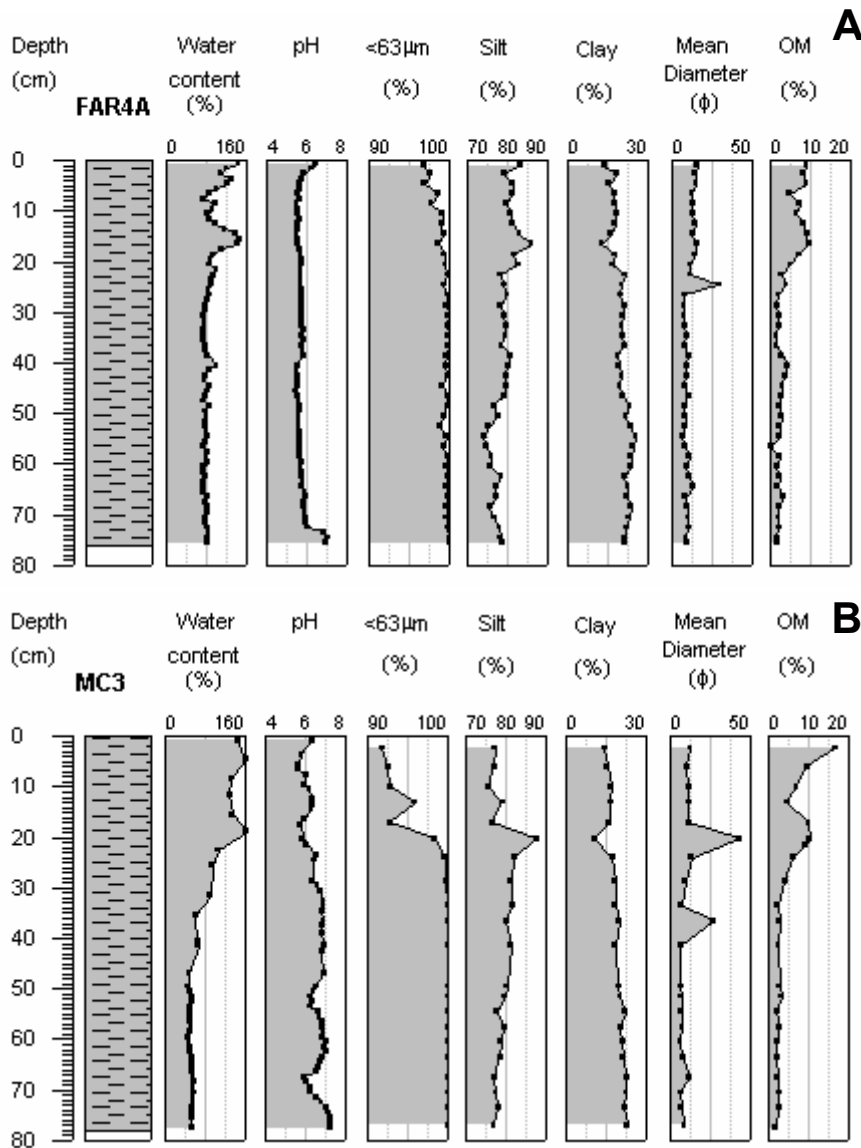
Fig. 4.– The vertical profiles of sedimentological properties. A – FAR4A core; B – MC3 core.
Fig. 4.– Perfiles verticales de los atributos sedimentológicos. A. sondeo FAR4A; B. sondeo MC3.

grain size ranges mainly between 4 and 8 μm (fine silt). Quartz particles (FAR4A) and plant remains (FAR4A and MC3) account for the residual sand (> 63μm) fraction. Despite the proximity of the Tróia dune complex, no wind-blown sand occurred in MC3. The mud is essentially sub-acid in FAR4A and sub-acid to neutral in MC3 (Fig. 4A, B). OM contents are low (<4 wt%) in consequence of the type and density of biomass typical of this environment and/or due to OM degradation. The water contents (taken shortly after collection) ranged between 60 and 87%, in agreement with a non consolidated state (Dunn *et al.*, 1980; Das, 1998).

The high marsh sediment also consists essentially of slightly clayey silt (<63μm fraction exceeding 92%); the silt fraction represents 75-88% of the total sediment and the clayey fraction decreases upwards. Sand-sized components increase upwards (especially in the top 20 cm) and are composed exclusively of plant debris at MC3

(including roots and rhizomes), excluding contribution of the adjacent dunes. At FAR4A both quartz sand and plant remains were found deeper than 15cm depth, but the former is absent in the top layer. In the top 20 cm the mean diameter of muddy particles also increases (10-15 μm - medium silt – some anomalous values may be due to the elongated shape of larger organic particles). The pH is still quite uniform at FAR4A but slightly increases between 40 and 20 cm, although the sediment is classified as sub-acid. At MC3, the pH values are more variable, the sediment being neutral until 30 cm depth and sub-acid in the topmost 30 cm (Fig. 4A, B). In both sites, pH increases in the sub-surface sediment layer reflecting the influence of marine water. OM content increases significantly, especially in the top 20 cm (in consequence of higher root density, less OM degradation), where it reaches 10 wt % and exceptionally 17 wt % in the superficial sample of MC3. Water contents increase upwards;

Core FAR4							Core MC3					
Sample	Depth (cm)	210Pb	±	137Cs	±		Sample	Depth (cm)	210Pb	±	137Cs	±
0.0-2.0	1	44	8	7	1		0.0-1.5	0.75	73	7	9	1
2.0-4.0	3	54	10	10	2		4.0-5.0	4.5	51	8	13	1
4.0-5.5	4.5	43	10	6	2		8.0-9.0	8.5	43	7	15	1
7.0-8.0	7.5	30	6	8	1		11.0-12.0	11.5	13	8	51	3
10.0-11.0	10.5	24	6	7	1		15.0-16.0	14.5	33	9	8	1
13.0-14.0	13.5	18	7	10	1		18.0-19.5	18.75	16	4	2	1
15.0-16.0	15.5	13	7	12	1		22.0-23.0	22.5	16	7	nd	-
17.0-18.0	17.5	11	3	31	1		25.0-26.5	25.75	5	5	nd	-
19.0-20.0	19.5	19	5	19	1		26.5-28.0	27.25	6	5	nd	-
22.0-23.0	22.5	1	0	nd	-		31.0-32.0	31.5	5	4	nd	-
25.0-26.0	25.5	6	5	nd	-							
28.0-29.0	28.5	1	0	-	-							
33.0-34.0	33.5	2	4	-	-							

Table 1. Data on excess 210Pb and 137Cs (activity - Beq/kg±1σ) in cores FAR4 and MC3.
Tabla 1. Valores en exceso para 210Pb y 137Cs (actividad - Beq/kg±1σ) en los sondeos FAR4 y MC3.

in the top 20 cm the water content exceeds 100%, due to a more open fabric imposed by rootlets and plant debris; two maxima in water content were found, close to surface and approximately 15 to 20 cm depth (Fig. 4A, B).

3.2. Geochemistry

Isotopes and sedimentation rates

The analytical results for 210Pb and 137Cs radionuclides in cores FAR4 and MC3 are shown in Table 1 and plotted in figures 5 and 6. Plotting excess 210Pb against depth (Fig. 5A and 6A) shows no signs of disturbance by near surface sediment mixing. The linear regression of the data indicates a sedimentation rate of 2.8 mmyear^{-1} at FAR4 and of 3.4 mmyear^{-1} at MC3 (Fig. 5A and 6A). The first appearance of 137Cs (Fig. 5B and 6B) in both marsh sediments has been detected at 19-20 cm depth and assumed to represent the earliest release of this radionuclide in the Northern Hemisphere, in 1954 (Delaune *et al.*, 1978, *in* Cearreta *et al.*, 2002). A single 137Cs maximum peak (considered to reflect the maximum of atmospheric deposition of this artificial radionuclide in consequence of a large amount of nuclear tests performed in 1963) is present at 17-18 cm depth in FAR4 and at 11-12 cm in MC3. At FAR4 the derived sedimentation rates range between 2.2 (1954-1963) and 4.4 (1963-2003) mmyear^{-1} and a bulk sedimentation rate of 4.0 mmyear^{-1} (1954-2003) can be computed with this radionuclide (Fig. 5B); at MC3 the equivalent sedimentation rates are 8.1 (1954-1963), 2.9 (1963-2003) and 3.8 mmyear^{-1} (1954-2003) (Fig. 6B). These figures agree reasonably with accumulation rates obtained from 210Pb and match values found in the lit-

erature for young high marsh environments (Pethick, 1984; Trenhaile, 1997; Woodroffe, 2002); no attempt to extrapolate these accretion rates for the low marsh environment has been undertaken given the varying (higher) orders of magnitude that can occur in the earlier stages of marsh development. Considering the sedimentation rates inferred from the 210Pb in FAR4 and assuming a uniform rate of sedimentation in the upper 30 cm, the 1963 marsh surface would correspond to an approximate depth of 12 cm; the vertical offset observed between this depth and the 18 cm corresponding to the same surface as interpreted from 137Ce may result from downward movement (molecular diffusion through pore water) of this radionuclide (cf. Geyh and Schleicher, 1990).

Elemental Analysis

In the studied FAR4A and MC3 cores, Si and Al contents range from 18 to 25 wt% and from 8 to11 wt% (Table 2 and 3), respectively (Fig. 7A, B), which are typical of muddy sediments. Si and Al contents and the clay/silt ratio decrease upwards, reflecting increasing abundance of OM. FAR4 OM values are lower than that those of MC3 due to a lower contribution of OM in the Faralhão marsh; this hypothesis is supported by consistent differences in LOI (a reliable proxy of the OM content) between the studied sites. Al and Si display positive correlations in both cores, suggesting that they were carried predominantly by particulate Al-silicates.

Higher Na contents occur within the upper 10-15 cm of both cores, and their concentration profiles mimic the variations of water contents, reflecting the infiltration and downcore intergranular diffusion of marine water (Fig.
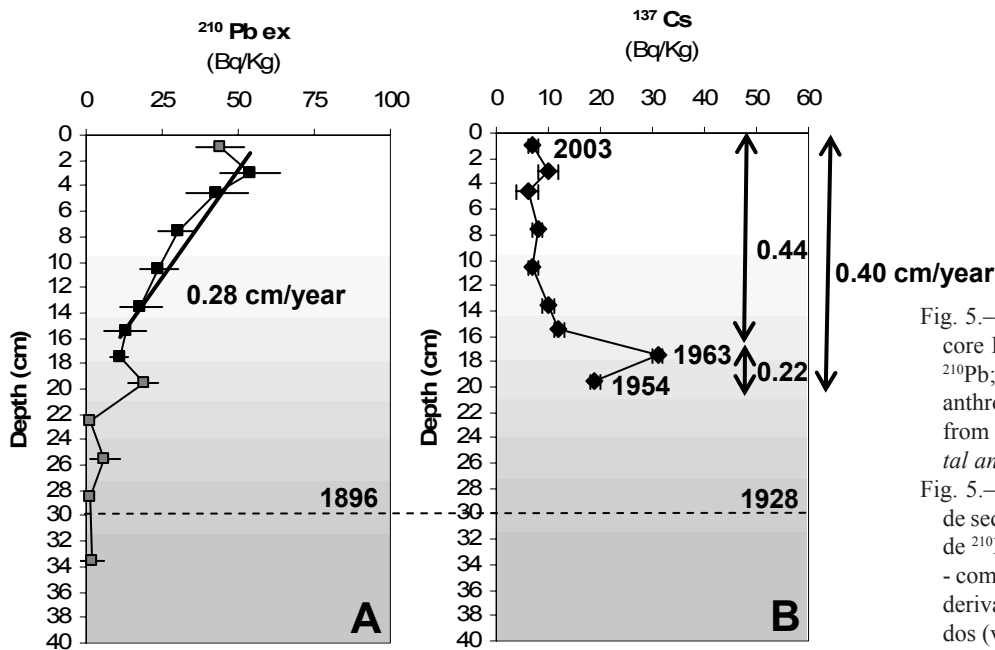
Fig. 5.– The vertival variation of radionuclides in core FAR4 and sedimentation rates. A - Excess ^{210}Pb; B – ^{137}Cs. Dashed line – beginning of anthropogenic signal in the sediment, derived from heavy metal concentrations (see *Elemental analysis*).

Fig. 5.– Variación vertical de los isótopos y tasas de sedimentación en el sondeo FAR4. A. Exceso de ^{210}Pb; B. Exceso de ^{137}Cs. Línea discontinua - comienzo de la señal antrópica en el sedimento derivada de la concentración en metales pesados (ver *Elemental analysis*).
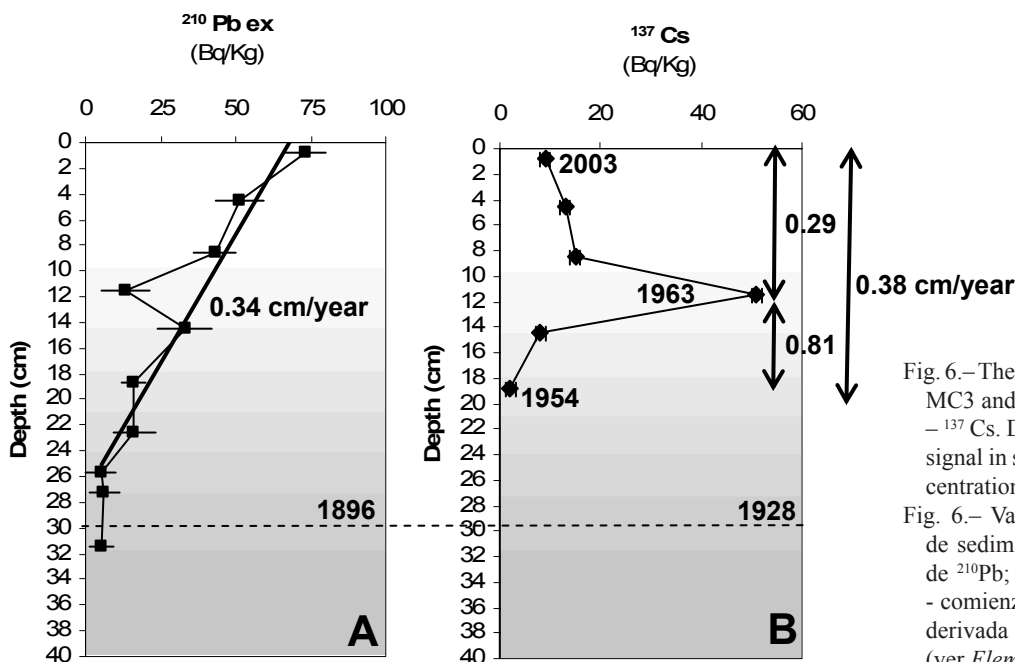

Fig. 6.– The vertical variation of radionuclides in core MC3 and sedimentation rates. A - Excess ^{210}Pb; B – ^{137}Cs. Dashed line - beginning of anthropogenic signal in sediment, derived from heavy metal concentrations (see *Elemental analysis*).

Fig. 6.– Variación vertical de los isótopos y tasas de sedimentación en el sondeo MC3. A. Exceso de ^{210}Pb; B. Exceso de ^{137}Cs. Línea discontinua - comienzo de la señal antrópica en el sedimento, derivada de la concentración en metales pesados (ver *Elemental analysis*).

7A, B). This was promoted by higher porosity and permeability, due to the presence of larger amounts of organic fragments in the upper sections of both cores. Indeed, factor analysis (Fig. 8A, B), shows that Na clusters with LOI in both cores. Higher MC3 sodium concentrations (compared to those of FAR4) are consistent with the higher water contents in MC3, due to higher OM and the open fabric.

The Ca contents are very low (0.1-0.7% – Tables 2 and 3), which is consistent with the relative acidity (6.9 > pH > 5.5) of the sediment and the absence of carbonate bioclasts (post depositional dissolution?) (Fig. 7A, B).

Ti and K concentrations are always higher in FAR4 marsh sediments when compared to those of MC3; K decreases towards surface in both field sites (Fig. 7A, B), whereas Ti follows no definite trend. Factor analysis (Fig. 8A, B) shows that K clusters with Al and Si (along Factor 1), suggesting an association of that element with aluminosilicates; in contrast, Ti shows no strong affinity with any other analysed element indicating a separate specific carrier for this element.

Fe shows a different behaviour in Faralhão and Malha da Costa marshes. At FAR4 site, Fe plots close to Mn and opposite to Al, K and Si (Fig. 8A), indicating precipita-

Depth (cm)	LOI %	Si %	Ti %	Al %	Fe %	Mn %	Mg %	Ca %	Na %	K %	Zn mg/kg	Cu mg/kg	Pb mg/kg
1.0	22.9	20.3	0.70	9.49	5.14	0.07	0.95	0.44	1.66	1.69	201	136	73
3.0	21.2	20.5	0.70	9.83	5.41	0.07	0.94	0.45	1.79	1.80	202	126	73
4.5	21.4	20.7	0.74	9.90	5.09	0.06	0.81	0.43	1.67	1.90	185	111	77
7.5	22.5	20.7	0.69	9.49	4.87	0.05	0.80	0.41	1.66	1.93	196	117	56
10.5	21.5	20.8	0.69	9.59	5.35	0.09	0.84	0.36	1.70	1.78	204	101	65
13.5	20.1	21.3	0.75	9.83	5.20	0.06	0.79	0.43	1.64	1.76	177	86	64
15.5	18.5	21.9	0.82	10.09	5.55	0.02	0.71	0.40	1.23	1.97	129	69	36
17.5	17.5	23.1	0.81	10.12	4.46	0.02	0.76	0.24	1.29	2.00	168	76	43
19.5	19.5	21.8	0.73	9.74	5.32	0.02	0.68	0.66	1.29	2.09	185	66	48
22.5	19.8	22.1	0.68	9.57	5.09	0.02	0.80	0.27	1.29	2.08	158	64	103
25.5	19.0	22.4	0.69	9.85	4.67	0.05	0.86	0.49	1.31	1.86	175	52	49
28.5	17.7	22.4	0.74	9.87	5.26	0.15	0.87	0.47	1.29	2.03	184	46	32
33.5	17.4	23.4	0.58	9.95	4.51	0.07	0.81	0.50	1.24	1.78	103	46	26
37.5	14.1											46	
41.5	14.5	23.7	0.82	10.65	4.94	0.09	0.86	0.28	1.18	1.94	77	45	26
47.0	14.2											42	
51.5	14.7	23.2	0.85	10.37	5.30	0.05	0.94	0.37	1.31	2.23	104	41	13
57.0	14.7											43	
62.5	15.8	23.8	0.79	10.41	3.98	0.02	0.83	0.34	1.22	2.19	87	40	171
67.6	15.5											43	
73.3	15.0											40	
78.5	14.1	23.9	0.65	10.74	4.45	0.02	0.84	0.45	1.32	2.19	67	51	104

Table 2. Compositional data of sediments cored in Faralhão.
Tabla 2. Composición de los sedimentos perforados en Faralhão.

Depth (cm)	LOI %	Si %	Ti %	Al %	Fe %	Mn %	Mg %	Ca %	Na %	K %	Zn mg/kg	Cu mg/kg	Pb mg/kg
0.8	30.4	18.2	0.41	7.89	4.47	0.04	1.25	0.43	3.31	1.25	218	64	38
4.5	30.3	18.4	0.48	8.45	3.74	0.05	1.23	0.11	3.44	1.16	136	58	39
8.5	24.1	20.8	0.49	8.88	4.28	0.03	1.19	0.36	2.78	1.22	161	54	38
11.5	24.7	20.7	0.66	8.23	4.62	0.04	1.18	0.38	2.73	1.32	169	55	41
15.5	24.4	21.0	0.64	8.63	4.12	0.04	1.13	0.26	2.62	1.28	261	60	33
18.8	27.6	20.0	0.57	7.76	4.19	0.05	1.21	0.29	2.82	1.35	165	52	16
22.5	21.4	22.0	0.63	8.95	4.23	0.04	1.17	0.54	2.23	1.46	154	43	35
25.8	19.4	22.7	0.59	9.30	4.43	0.04	1.23	0.44	2.00	1.50	133	40	33
27.3	19.4	23.7	0.62	8.69	4.10	0.03	1.15	0.15	1.90	1.49	126	39	31
31.5	18.7	22.9	0.68	9.46	4.78	0.03	1.15	0.41	1.59	1.53	113	38	35
35.5	16.3	25.2	0.63	8.45	4.81	0.04	1.10	0.33	1.44	1.38	105	39	32
47.0	15.2										116	36	
50.5	16.1	23.4	0.64	9.57	5.01	0.04	1.32	0.45	1.80	1.79	107	42	37
54.5	15.0										107	39	
57.5											102	44	
59.5	13.4	23.8	0.56	10.73	5.17	0.04	1.29	0.29	1.76	1.76	106	37	36
63.5	15.6										99	42	
67.5	16.1										89	39	
69.5	14.1	24.2	0.51	10.43	4.59	0.03	1.22	0.46	1.79	1.53	98.9	38	34
72.5	16.7										87	40	
76.5	15.4	24.5	0.48	9.95	4.52	0.05	1.24	0.18	1.53	1.49	95	38	33

Table 3. Compositional data of sediments cored in Malha da Costa.
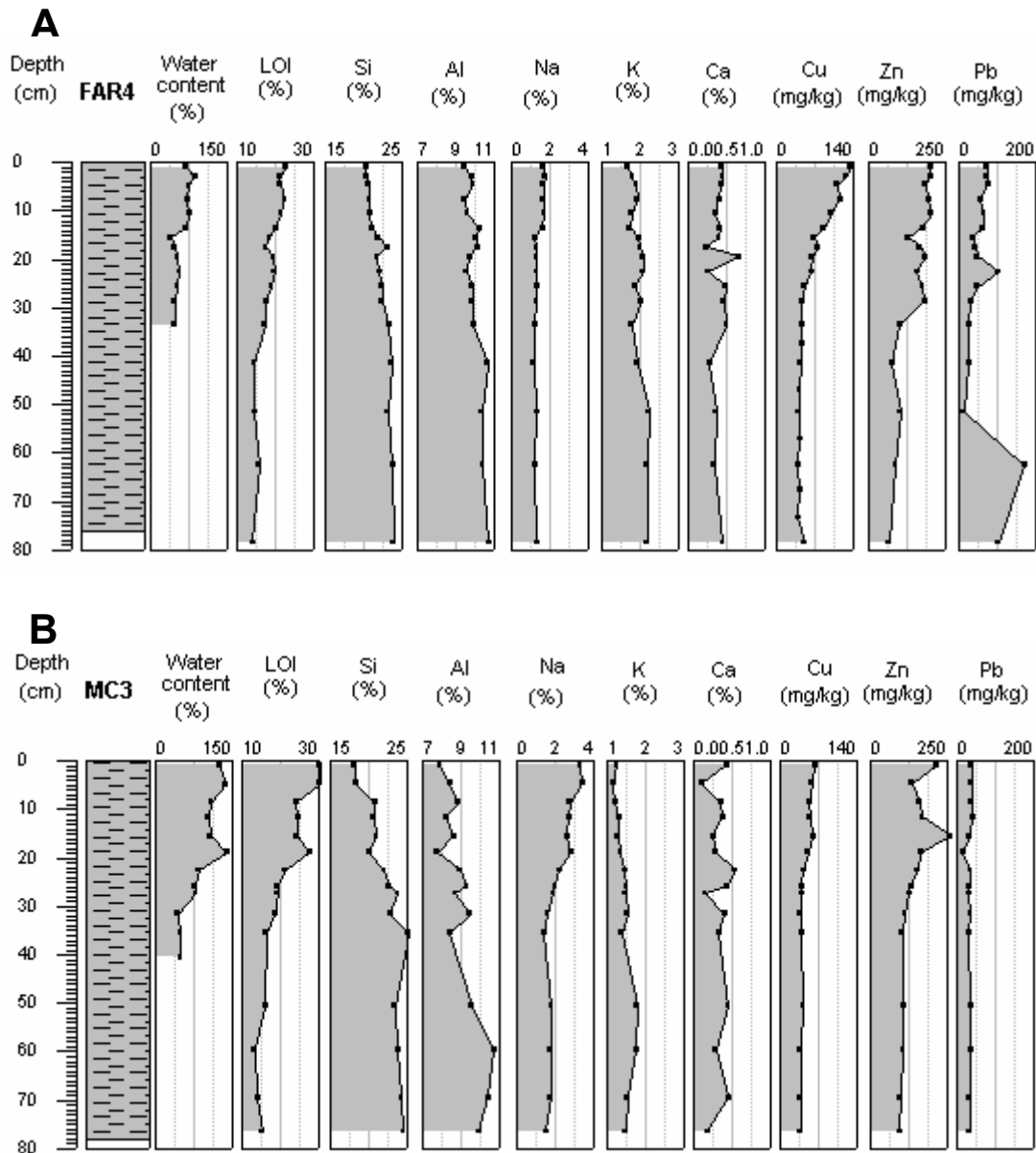Tabla 3. Composición de los sedimentos perforados en Malha da Costa.

Fig. 7.– The vertical variation of water content, LOI and geochemical elements. A – FAR4A core; B – MC3 core.
Fig. 7.– Perfiles verticales del contenido de agua, LOI y elementos geoquímicos. A. sondeo FAR4; B. sondeo MC3.

tion as oxides/hydroxides; the overall co-variation trends exhibited by Fe/Al, Cu/Al and Zn/Al ratios (Fig. 9), also suggest that adsorption by Fe-oxides may have been responsible for heavy metal influx into FAR4 sediments. In contrast, at the MC3 site, Fe clusters with Al, K and Si (Fig. 8B), suggesting a significant association with the aluminosilicate component.

Depth - element concentration profiles for heavy metals (Cu, Zn and Pb) in figure 10 show a clear boundary between two different geochemical domains (see also Table 4): a lower section (below ~30 cm depth), where heavy metal contents are lower and more homogeneous, with the exception of two outliers in Pb at FAR4 for which no explanation was found so far, and an upper section typi-

cally enriched in heavy metals. The upper section of the Faralhão marsh has higher heavy metal concentrations (particularly, Cu and Zn) than those of equivalent samples in the Malha da Costa and Cu and Zn display higher contrast between both sections in comparison with Pb.

Heavy metal contents in the deeper (> 30 cm depth) sections of both cores compare favourably with those of typical continental crust sediments (e.g., Salomons and Förstner, 1984; Taylor and McLennan, 1985) and international reference material (Average Shale) (Salomons and Förstner, 1984) (Fig. 10) and may be taken as representative of their respective geochemical background values.

The small textural variability in the marsh sediment illustrated by the poor to negative correlation between the

Core FAR4			
	Cu (mg/kg)	Zn (mg/kg)	Pb (mg/kg)
0 – 30 cm	46 – 136	129 – 204	26 – 103
30 – 84 cm	40 - 51	67 – 104	13 - 26

Core MC3			
0 – 30 cm	39 – 64	126 – 261	16 – 41
30 – 78 cm	36 - 44	87 – 116	32 - 37

Table 4. Minimum and maximum concentration values of Cu, Zn and Pb in lower (background) and upper (enriched) sections obtained in cores FAR4 and MC3.

Tabla 4. Concentraciones máximas y mínimas de Cu, Zn y Pb en las secciones inferior (no contaminada) y superior (enriquecida) de los sondeos FAR4 y MC3.

metal and Al contents precludes the need of normalization in relation to this element.

Except for Pb in MC3, LOI values display an overall positive correlation with heavy metal concentrations ($r^2_{Zn-LOI} = 0.91$; $r^2_{Cu-LOI} = 0.87$) in both cores due to the affinity between metals and OM; therefore, normalization of heavy metal relative to LOI contents has been undertaken (Fig.11). The similar shape of the vertical heavy metal content profiles (before and after normalization), obtained at FAR4 indicates that the variations in OM can not be accountable for increasing heavy metal contents in the upper section of the core. However, in MC3, normalization of heavy metal contents against LOI values shows more homogeneous profiles, suggesting limited availability of heavy metals, such that their concentrations in the sediments may have been partially buffered by enhanced adsorption by OM. Accordingly, MC3 upper section heavy metal enrichment factors (relative to background values, computed using LOI) are close to unity, whereas the upper section heavy metal enrichment at FAR4 is
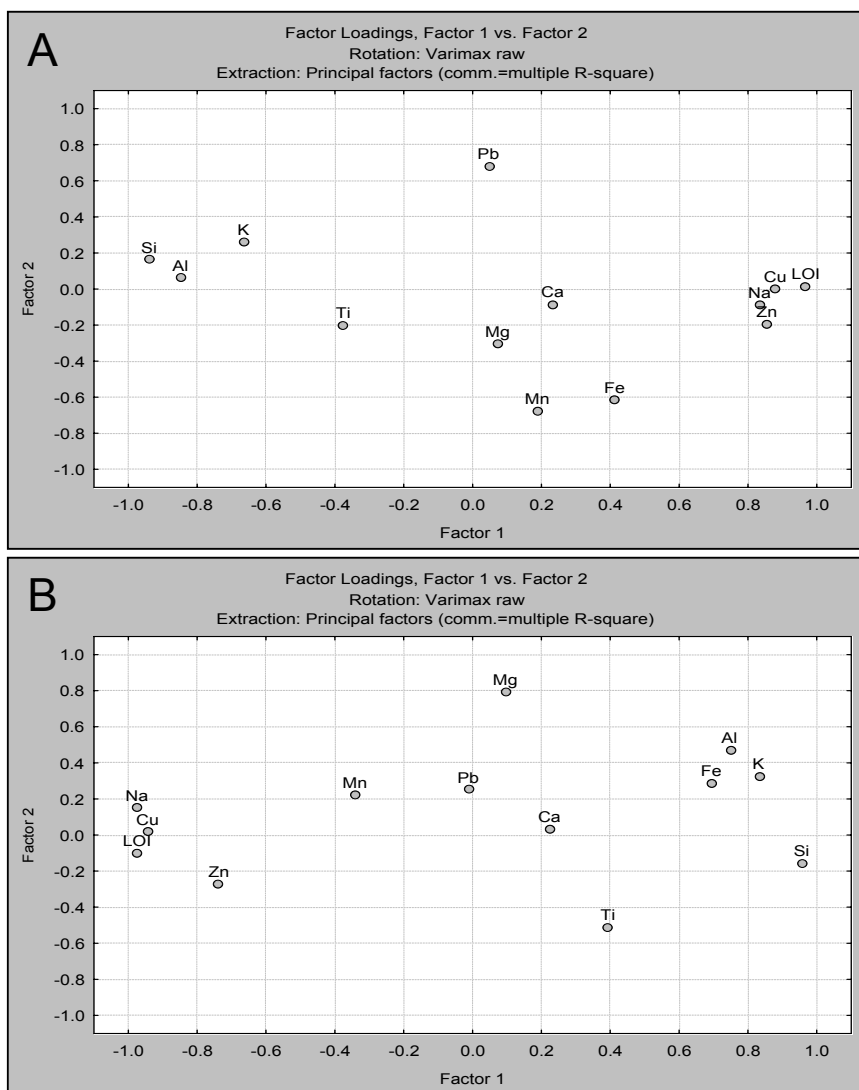

Fig. 8.– The results of Factor Analysis. Plot of LOI and geochemical elements along Factors 1 and 2. A – FAR4A core; B – MC3 core.

Fig. 8.– Resultados del Análisis de Factores. Representación de LOI y de elementos geoquímicos a lo largo de los factores 1 y 2. A. sondeo FAR4; B. sondeo MC3.
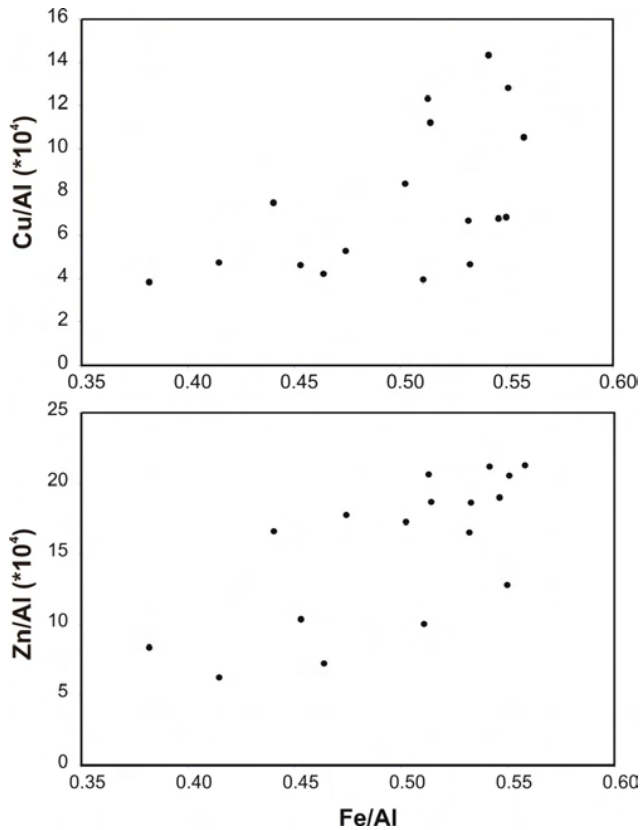
Fig. 9.– Plots of Cu/Al and Zn/Al (* 10^4 g/g) against Fe/Al ratios for FAR4 core, illustrating the association of heavy metals with iron oxides at this site.

Fig. 9.– Representación de Cu/Al y Zn/Al (* 10^4 g/g) *versus* Fe/Al en FAR4, ilustrando la asociación de metales pesados con óxidos de hierro.

Fig. 10.- Vertical variation of heavy metal contents in both coring sites. Dotting line – metal content in the Average Shale (Salomons and Förstner, 1984)). Dashed line – metal content in mean sediment (Salomons and Förstner, 1984).

Fig 10.– Variación vertical del contenido de metales pesados en ambos puntos de sondeo. Línea punteada - contenido medio de metales en Average Shale (Salomons and Förstner, 1984). Línea discontinua – contenido medio de metales en sedimentos de la corteza continental (Salomons and Förstner, 1984).

systematically > 1 (1.5, 1.6 and 2.1 for Cu, Zn and Pb, respectively; Table 5). The contrasting relationships between heavy metal and LOI contents at the studied sites are well illustrated in figure 12; at FAR4 site high and positive increasing rates of Cu and Zn contents per unit mass of LOI indicate that (relative) heavy metal influx was largely in excess to that of OM, whereas at MC3 site the lower variation rates, as well as the parabolic dCu/dLOI, dZn/dLOI vs. LOI trends towards negative values at high LOI contents (representing the uppermost section of the core), clearly demonstrate the reduced availability of heavy metals at this site. The resulting distinct geochemical patterns clearly reflect an asymmetrical influx of heavy metals into the recent sediments of the estuarine high marsh.

The vertical variations in the behaviour of heavy metals is analysed in figure 13, by plotting heavy metal contents in excess of those of their respective (average) background values ($\Delta c(M)_i = c(M)_i - c_{average} (M)_{background}$: see above) against depth, for both cores. The observed geochemical patterns are complex (Fig. 13), displaying distinct trends for different elements at both sites. However
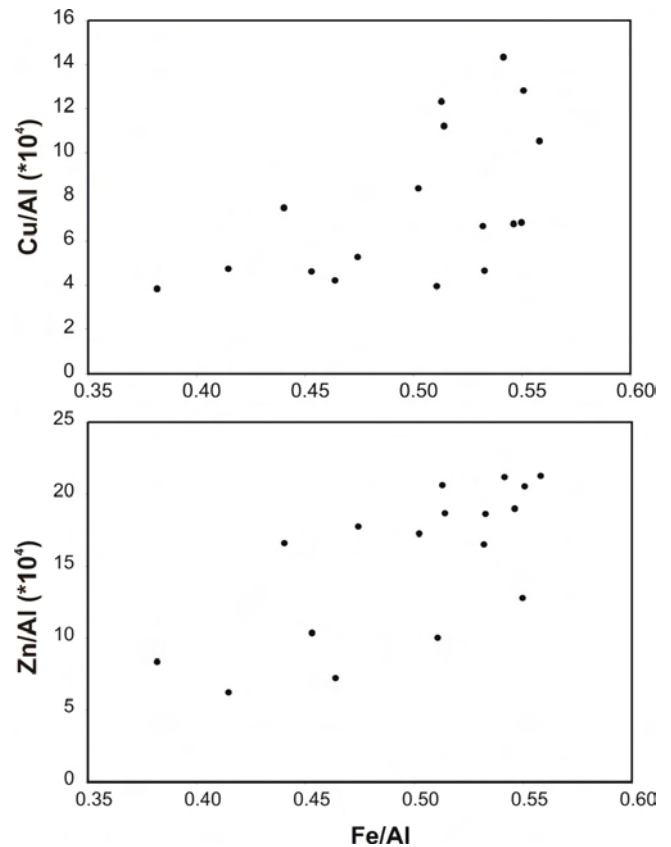
Core FAR4

	Cu	Zn	Pb	LOI
0 – 30 cm	88	180	60	20
30 – 84 cm	44	88	22	15
EF (0-30 cm)	1.5	1.6	2.1	-
EF (0-13.5 cm)	1.8	1.6	2.3	-
EF (13.5-30 cm)	1.1	1.6	2.0	-

Core MC3

	Cu	Zn	Pb	LOI
0 – 30 cm	52	169	34	25
30 – 78 cm	39	102	35	16
EF	0.8	1.1	0.6	-

Table 5. Average concentration values of Cu, Zn, Pb and LOI in lower section (uncontaminated) and upper section (enriched) obtained in cores FAR4 and MC3 and Enrichment Factors (EF) for these metals.

Tabla 5. Concentraciones medias de Cu, Zn, Pb y LOI en las secciones inferior (no contaminada) y superior (enriquecida) de los sondeos FAR4 y MC3, y Factores de Enriquecimiento (EF) para estos metales.
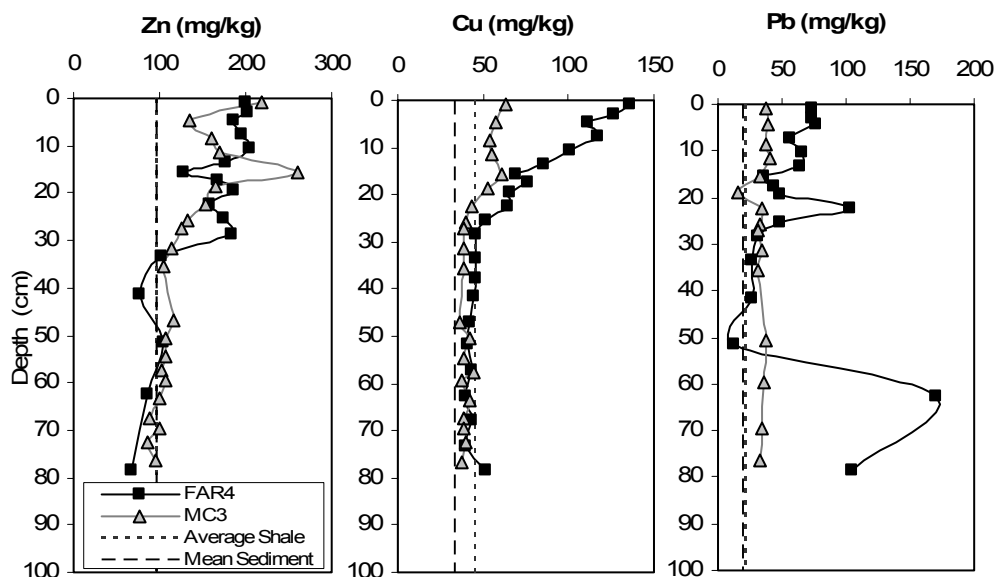
Fig. 11.– Vertical variation of heavy metal contents in both coring sites normalized by LOI.

Fig. 11.– Variación vertical del contenido de metales pesados en ambos puntos de sondeo normalizado por el LOI.
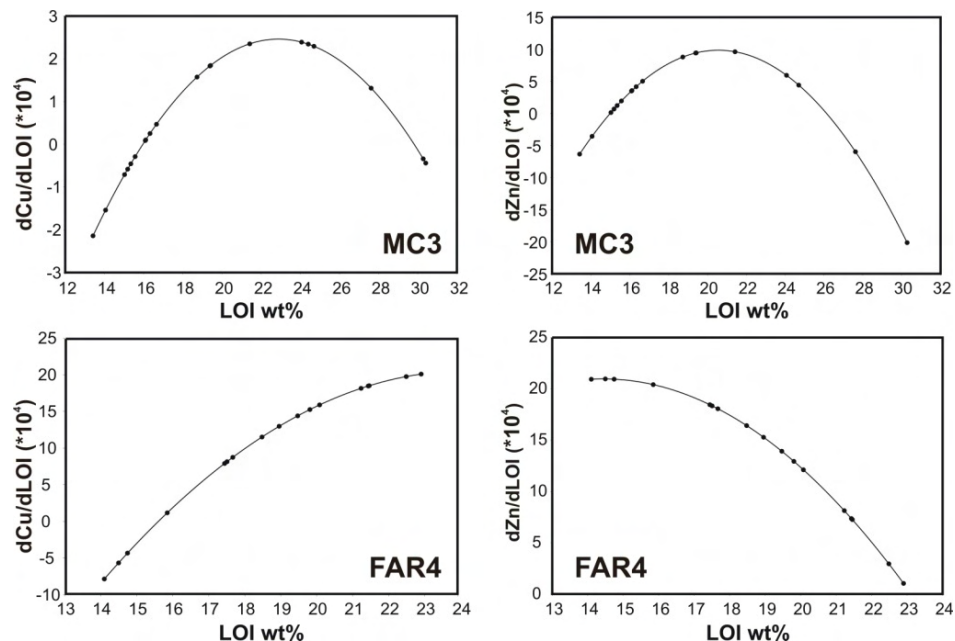

Fig. 12.– The Cu and Zn content variation rates per unit mass variation of LOI (* 10^4 g/g) plotted against LOI wt %, at FAR4 and MC3 sites.

Fig. 12.– Tasas de variación del contenido en Cu y Zn por variación de unidad de masa de LOI (* 10^4 g/g) *versus* LOI wt %, en FAR4 y MC3.

(except for undefined scattering of a few Pb values; not shown), Cu and Zn show relatively homogeneous $\Delta c(M)$ (~ 0) values within the lower sections (> 30 cm depth) of both cores, strongly suggesting that the observed $\Delta c(M)$ variations at shallower levels may be ascribed to variable (time related) anthropogenic influence in the area.

Indeed, sedimentation rates derived from radionuclides allow definition of the earliest anthropogenic signal in marsh sediments to extend from the first two decades of the 20th century (Fig. 5 and 6) at ~ 30 cm depth, which is consistent with the geochemical inferences discussed above. This time interval (1900-1920) precedes the boom of urban and industrial development of the Setúbal area (which occurred in the 1960's) and we suggest that the in-

itial increase of heavy metal $\Delta c(M)$ values (Fig. 13) was related, in both marshes, to a contemporaneous increase in the exploitation and processing of pyrite ore, further upstream in the Sado basin, which occured after 1866-1875 (Cruz, 2007). Following the common initial 1900–1920 anthropogenic signal, $\Delta c(M)$ – depth variations are different for the two studied sites, with much higher and steadily increasing $\Delta c(M)$ values at FAR4 (Fig 13). Thus, sedimentation rates (determined with radionuclide geochronological data; Fig. 5 and 6) were coupled with $\Delta c(M)$ – depth results displayed in figure 13 in order to obtain a (first-order) assessment of anthropogenic heavy metal flux patterns into both sites, since 1900 – 1920. Fluxes are expressed as heavy metal mass input per cm
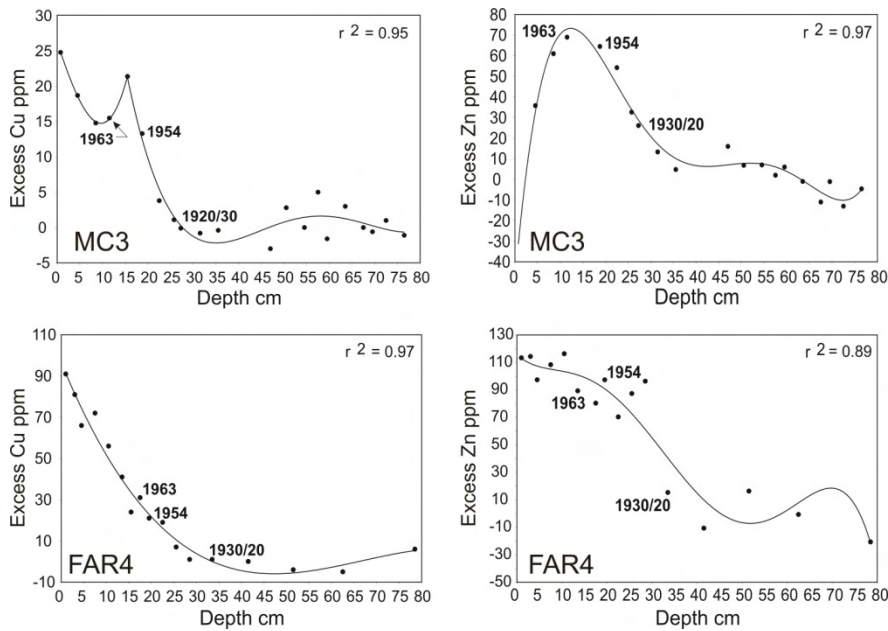
Fig. 13.– Excess Cu and Zn concentrations (relative to average background contents; see text) plotted against depth (cm) for FAR4 and MC3 core samples. Best-fit regression lines (plus r² values) and controlling dates (determined by radionuclide dating) are also shown in the diagrams.

Fig. 13.– Concentración de Cu y Zn en exceso (relativo a valores de fondo locales) *versus* profundidad en FAR4 y MC3, curvas de mejor ajuste, valores de r² y fechas de control (obtenidas a partir de isótopos).
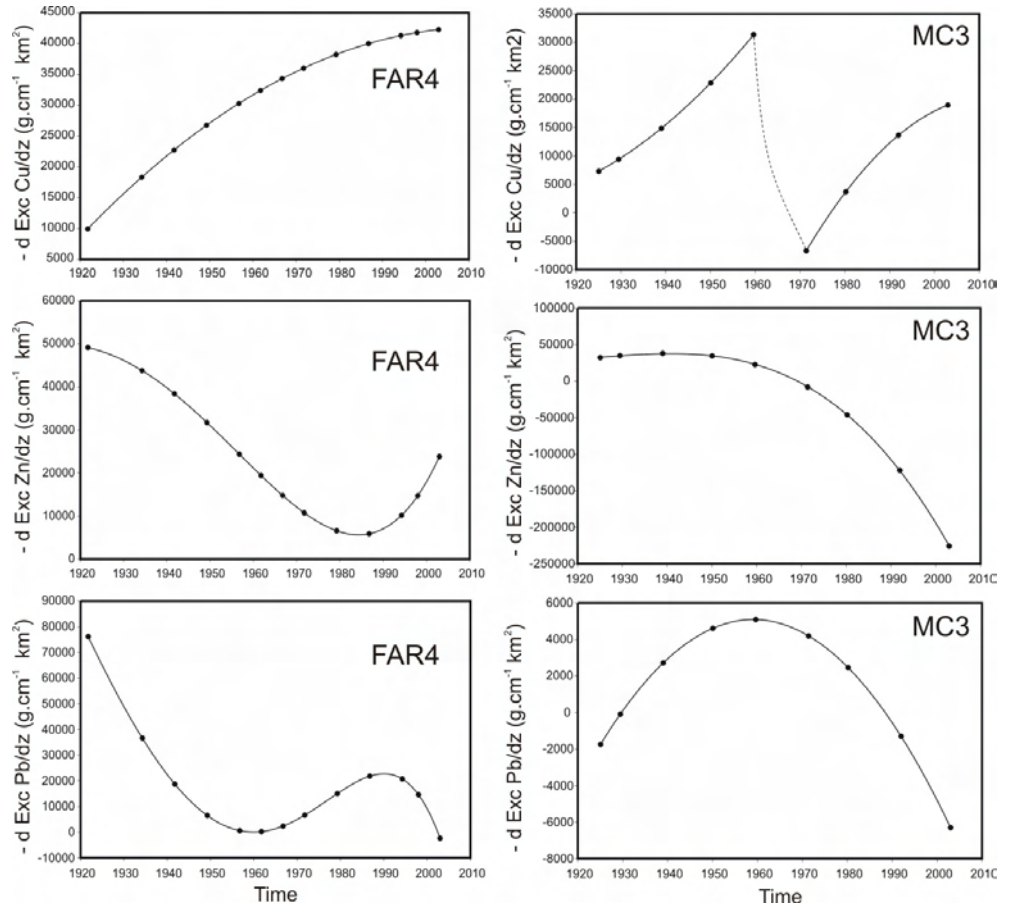

Fig. 14.– The variations of excess Cu, Zn and Pb ("anthropogenic") fluxes per cm of deposited sediment (see text) plotted against time for FAR4 and MC3 sites.

Fig. 14.– Variación del exceso de flujo de Cu, Zn y Pb antropogénico por cm de sedimento acumulado *versus* tiempo en FAR4 y MC3.

sediment deposition (g. cm⁻¹) at each time, normalized to an area of 1 km², as displayed in figure 14. The obtained results are consistent for both sites and (except for Cu in FAR4) indicate an overall break in heavy metal fluxes into the marsh sediments at ~1960-1980. This is interpreted as being due to contemporaneous reinforcement

of mining environmental controls and the decay of the exploitation of base metals in the Iberian Pyrite Belt, which significantly decreased the heavy metals influx into the Sado drainage basin. Nevertheless, heavy metal fluxes are clearly distinct at both sites: at MC3 absolute values of heavy metal inputs are generally lower and Zn
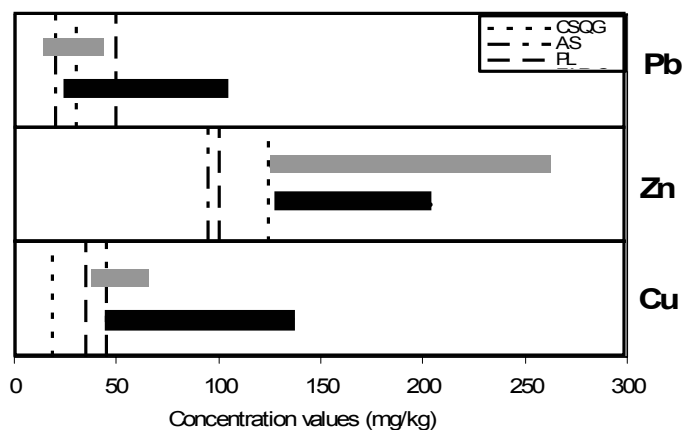
Fig. 15.- Range of metal concentrations in the enriched upper section of the sediment of Faralhão (black rectangle) and Malha da Costa (grey rectangle) marshes, compared with reference values. CSQG – target values of Canadian Sediments Quality Guidelines; PL – maximum value for clean sediments in Portuguese legislation for dredged materials; AS – metal content in Average Shale.

Fig. 15.– Rango de las concentraciones de metales en el sector superior enriquecido de las marismas de Faralhão (rectángulo negro) y Malha da Costa (rectángulo gris) comparado con los valores de referencia. CSQG- valores fijados por la Directriz de Calidad de Sedimentos Canadiense; PL- valor máximo para sedimentos limpios según la legislación portuguesa sobre material dragado. AS- Contenido de metales en Average Shale.

and Pb fluxes steadily decrease from ~1960 to the present time (leading to $\Delta c(M) < 0$); whereas at FAR4 there is no 1960 – 1980 break in Cu fluxes (which continuously increase from 1920 to the present time) and Zn, Pb fluxes rapidly recover, reflecting intensification of industrial (and farming?) activities in the area after 1960 – 1970. The uppermost inflexion to lower Pb fluxes (1995-2000) observed in FAR4 (Fig. 14), may result from the widespread consumption of unleaded gasoline. The different degree of anthropogenic pollution at the two sites is clearly illustrated by the contrasting cumulative amounts of heavy metals that were accumulated in the marsh sediments since 1900-1920: 3.7 Cu, 13.3 Zn and 0.4 Pb ton. km^{-2} at MC3; 11.5 Cu, 29.2 Zn and 11.7 Pb ton.km^{-2} at FAR4 (considering sediment bulk dry weight 1000 kg/m^3 and the section area of the sampler representative of the marsh). These differences most probably reflect distinct sedimentation conditions, related with relative proximity to industrial pollution sources at FAR and much more efficient material flushing into estuarine waters at the MC site.

Nevertheless, heavy metal concentrations in the upper (enriched) section of both Faralhão and Malha da Costa marshes are, in general, higher when compared with the Average Shale International Reference and with target values in the Canadian Sediments Quality Guidelines (2002) and with values indicated for clean sediments in

the Portuguese legislation for dredged materials (DR nº 141 – II Série – 21/06/95) (Fig. 15). Given that the heavy metals fixed by sediments should represent only a small percentage of the total anthropogenic input into the Sado estuary, a large amount of pollutants remains available for incorporation into the food chain, implying that the new data obtained from the studied sites should deserve environmental concern.

5. Conclusions

The sediments of the salt marshes of Faralhão and Malha da Costa, in the Sado estuary, are uniform in texture and are fine-grained, generally acid, with high values of organic matter in the topmost 20 cm and are free of bioclasts. Sand sized particles are rare and essentially made of coarse plant remains, although some quartz has been found, especially at Faralhão.

Sedimentation rates in the high marsh derived from ^{210}Pb and ^{137}Cs are in the order of 2-4 mm year^{-1} for the last 50 years in both sites but higher values can be found during shorter time intervals.

Si and Al contents are typical of muddy sediments and both elements correlate positively, suggesting an aluminosilicate carrier. The vertical variation in Na reflects infiltration and diffusion of marine water, whereas very low Ca contents are related to the absence of carbonate bioclasts. Heavy metals including Fe are associated with adsorption by oxides/hydroxides at FAR4, whereas at Malha da Costa (MC3) Fe shows affinity with aluminosilicates.

Vertical concentration profiles of heavy metals Cu, Pb and Zn, indicate enrichment in the top 30 cm of the high marsh sediment, which accumulated since 1900-1920; in the underlying sediment the metal content is similar to the Average Shale International Reference. Cu and Zn show a higher contrast between the upper and lower sections in comparison with Pb; enrichment is always higher in the Faralhão marsh, with factors of 1.5, 1.6 and 2.1 for Cu, Zn and Pb, respectively, whereas at Malha da Costa they are close to unity, indicating a contrast of spatial distribution of metals along the estuarine margins.

The earliest increase in metal concentration can be related to the intensification of exploitation and processing of pyrite ore in the Sado drainage basin at 1900-1920. There is a break in metal influxes around 1960-1980, which is interpreted as the result of decaying base metal exploitation in the Iberian Pyrite Belt and contemporaneous increasing of environmental concerns and legislation. At FAR4 this break is followed by a local increase of heavy metal fluxes, which is related to intensification of industry and farming (?), which is mostly located on the

north margin (Faralhão) of the Sado estuary.

The concentration of metals in the enriched upper parts of the sediments at both marshes exceeds the recommended target values indicated in quality guidelines (both Portuguese and Canadian), suggesting the need for environmental concern within the studied area.

Acknowledgements

References

Andrade, C., Freitas, M.C., Brito, P., Amorim, A., Barata, A., Cabaço, G. (2006): Estudo de Caso da Região do Sado. Zonas Costeiras. In: F.D. Santos, P. Miranda (eds), *Alterações Climáticas em Portugal – Cenários, impactos e medidas de adaptação*. Projecto SIAM II, Gradiva, Lisboa, Portugal: 389-479.

Belchior, F., Vale, C., Drago, T., Gil, O., Madureira, M.J. (2000): Relação entre contaminantes, alumínio e matéria orgânica nos sedimentos do estuário inferior do Sado. IX *Sem. Ibérico de Química Marinha, Estudos de Biogeoquímica na Zona Costeira Ibérica*, Univ. Aveiro: 227-234.

Canadian Environmental Quality Guidelines (2002): Canadian Council of Ministers of the Environment, 1999, updated 2001, updated 2002. In: http://www.ec.gc.ca/ceqg-rcqe/English/ceqg/sediment/default.cfm

Cearreta, A., Irabien, M. J., Ulibarri, I., Yusta, I., Croudace, I. W., Cundy, A. B. (2002): Recent salt marsh development and natural regeneration of reclaimed areas in the Plentzia estuary, N Spain. *Estuarine, Coastal and Shelf Science*, 54: 863-886.

Cortesão, C., Vale, C. (1995): Metals in sediments or the Sado estuary (Portugal). *Marine Pollution Bulletin*, 30, 1: 34-37.

Costa, J.B. (1999): *Caracterização e Constituição do Solo*. Fund. Cal. Gulbenkian. 4ª ed., 527p.

Cruz, I.(2007): Cobre na mineração em Portugal – o tempo das pirites. Centro interdisciplinar de Ciência da Universidade de Lisboa. http://www.triplov.com/Isabel_cruz/cobre/minas1.html (consulted in 29/6/2007).

Das, B.M. (1998): *Principles of Geotechnical engineering*. PWS Publishing Company, Boston, 712p.

Davis Jr, R. A., FitzGerald, D. M. (2004): *Beaches and coasts*. Blackwell Publishing, Oxford, U.K, 419 p.

Dias, J. A., Taborda, R. (1992): Tidal Gauge Data in Deducing Secular Trends of Relative Sea Level and Crustal Movements in Portugal. *Journal of Coastal Research*, 8: 655-659.

Dunn, I.S., Anderson, L.R., Kiefer, F.W. (1980): *Fundamentals of geotechnical analysis*. John Wiley & Sons, Inc., New York, 414 p.

Flemming, B.W. (2000): A revised textural classification of gravel-free muddy sediments on the basis of ternary diagrams. *Continental Shelf Research,* 20: 1125-1137.

Geyh, M. A., Schleicher, H. (1990): *Absolute age determination. Physical and chemical dating methods and their application*. Springer Verlag, 503p.

Head, K. (1980): *Manual of soil laboratory testing*. Volume 1: Soil classification and compaction tests. Pentech Press, London.

I H - Instituto Hidrográfico (1999, 2000): *Relatório Técnico* REL. TF QP. Instituto Hidrográfico, Divisão de Química e Poluição do Meio Marinho, Lisboa.

LNEC (1967): Standard E-201 – Solos – *Determinação do teor em matéria orgânica*. Documentação Normativa, 3p.

Loring, D.H., Rantala, R.T.T. (1992): Manual for the geochemical analyses of marine sediments and suspended particulate matter. *Earth-Science Reviews*, 32: 235-283.

Moreira, M. E. (1992): Recent salt marsh changes and sedimentation rates in the Sado estuary, Portugal. *Journal of Coastal Research*, 8: 631-640.

Pêra, M.T., Cunha, M., Barros, M., Dias, A. (1977): Concentração de metais pesados nos sedimentos das zonas do estuário do Sado usadas para cultivo de ostras. *Com. Serv. Geol. de Portugal*, tomo LXII: 85-134.

Pethick, J. (1984): *An introduction to coastal geomorphology*. Edward Arnold, 260 p.

Quevauviller, P., Lavigne, R., Cortez, L. (1989): Impact of Industrial and mine drainage wastes on the heavy metal distribution in the drainage basin and estuary of the Sado river (Portugal). *Environmental Pollution*, 59: 267-286.

Sousa, M. J. (2006): Contribuição para a caracterização geoambiental de sapais do estuário do Sado – aplicação experimental no ensino da Geologia. Master Thesis, New University of Lisbon, 309p.

Salomons, W., Förstner, U. (1984): *Metals in the hydrocycle*. Springer-Verlag, Berlin, 349 p.

Taylor, S. R., McLennan, S. M. (1985): *The Continental Crust: its composition and evolution*. Blackwell Scientific Publishers, Oxford.

Trenhaile, A.S. (1997): *Coastal dynamics and landforms*. Clarendon Press, Oxford, 366 p.

Vale, C., Sundby, B. (1980): A survey of the elemental composition of bottom sediments in the Sado estuary. Actual Problems Of Oceanography In Portugal. *Seminário organizado pela Junta Nacional de Investigação Científica e Tecnológica e Nato Marine Sciences Panel*, Lisboa, p.189-200.

Woodroffe, C. D. (2002): *Coasts. Forms, process and evolution*. Cambridge University Press, Cambridge UK, 623 p.